

Preliminary Design Review

In fulfillment of the NASA University Student Launch Initiative requirements



University of Illinois at Urbana-Champaign

Illinois Space Society (ISS)

104 S Wright Street
Urbana, Illinois 61801

Todo list

| | |
|-------------------------------------------------------------------------------------------------------------------------------------------------------------------------------------------------------------------------------------------------------------------------------------------------------|----|
| Add administrative and financial officers | 3 |
| Draft team-derived requirements | 22 |
| Expand on deployment requirements (robustness, rapidity) and ground proximity considerations . . . | 24 |
| Expand on descent phase, including trade-offs between guidance algorithms ((N)MPC, GPC) and waypoint tracking vs. visual guidance at close proximity (CV). | 24 |
| Expand on loiter phase, highlighting energy efficiency and data acquisition (feature detection and path planning) during idle phase. Also detail what safety features must be incorporated into this phase (geofencing, no-fly zones have to default back to loiter). | 24 |
| Expand on final approach and landing phase, including close-quarters operations and the role of computer vision in detecting the landing site, as well as the accuracy and terminal touch down conditions (velocity, attitude). Explain touch-and-go maneuvers in case of failed landing attempt. . . | 24 |
| Expand on retrieval protocol, including claw operations and validation of claw contents. Explain the details on distancing and safe idle mode after retrieval, as well as shutdown/hibernation routines. | 24 |
| Add sec. on hazardous operations | 37 |
| Add sec. on risk mitigation | 37 |
| Add sec. on hazardous materials | 37 |

List of Figures

| | |
|------------------------------------------------------------------|----|
| 5.1 VFR aeronautical chart of the Hazel Green, AL area | 21 |
|------------------------------------------------------------------|----|

List of Tables

| | | |
|-----|-------------------------------------------------------------------------------------------------------------------------------------|----|
| 7.1 | Simulation parameters | 32 |
| 7.2 | Maximum state deviation values for use in the $\bar{\mathbf{Q}}_1$ matrix in the Linear Quadratic Regulator (LQR) routine | 33 |
| 9.1 | Level of risk and member requirements | 39 |

ACKNOWLEDGEMENT

| <u>AREA</u> | <u>NAME/FUNCTION</u> | <u>SUBTEAM</u> |
|------------------------------------------|---------------------------------------------|-----------------------|
| Parts I, II, VI | H. El-Kebir <i>Team Lead</i> | — |
| Part III <i>Vehicle configuration</i> | G. Petrov <i>Subteam Lead</i> | Structures & Recovery |
| Part III <i>Avionics</i> | M. Bourla <i>Subteam Lead</i> | Avionics |
| Part III <i>Flight simulations</i> | R. Filipiuk <i>Subteam Lead</i> | Flight Dynamics |
| Part IV <i>Payload configuration</i> | K. Tochihara <i>Project Manager</i> | Payload |
| Part IV <i>Control systems</i> | A. Yaraneri <i>Chief Engineer</i> | Payload |
| Part V | Z. Essmyer <i>Ancillary Subteam Lead</i> | Ancillary |

HE: Add administrative and financial officers

It is requested that any organizations having specific comments in their area of responsibility contact the individual(s) listed above.

Acronyms

ATC Air Traffic Control. [46, 48](#)

BEMT Blade Element Momentum Theory. [17](#)

CDR Critical Design Review. [9](#)

CFD Computational Fluid Dynamics. [17, 27](#)

CM Center of Mass. [26](#)

CONOPS Concept of Operations. [9](#)

EIA Environmental Impact Assessment. [9](#)

EMST Electric Multirotor Sizing Tool. [17](#)

FAA Federal Aviation Authority. [20, 21, 23, 45, 46, 48, 49](#)

FMEA Failure Modes and Effects Analysis. [9](#)

FPV First Person View. [45](#)

ISS Illinois Space Society. [9](#)

LOS Line of Sight. [21, 23](#)

LQR Linear Quadratic Regulator. [2, 7, 33](#)

MAV Micro Air Vehicle. [17](#)

MIMO Multiple Input Multiple Output. [33](#)

MoI Moment of Inertia. [26](#)

NAR National Association of Rocketry. [20, 37, 38, 43](#)

PDR Preliminary Design Review. [9, 11](#)

PHA Personnel Hazard Analysis. [9](#)

RAC Risk Assessment Code. [39](#)

RMS Root Mean Square. [33](#)

RSO Range Safety Officer. [21](#), [24](#)

ToI Tensor of Inertia. [26](#), [27](#)

TRA Tripoli Rocketry Association. [37](#)

TSA Transportation Security Administration. [46](#)

UAS Unmanned Aerial System. [45](#), [46](#)

UAV Unmanned Aerial Vehicle. [11](#), [17](#), [18](#), [21–27](#), [32](#), [33](#), [45](#)

VFR Visual Flight Rules. [21](#)

ZENITH Zenith Estimation through Numerical Integration and Tractable Heuristics. [14](#)

ZOH Zero-order Hold. [31](#)

Contents

| | |
|--------------------------------------------|-----------|
| List of Figures | 1 |
| List of Tables | 2 |
| Acknowledgement | 3 |
| Glossary | 5 |
| Contents | 6 |
| 1 Preface | 9 |
| I Summary | 10 |
| 2 Executive Summary | 11 |
| II Changes | 12 |
| III Launch Vehicle | 13 |
| 3 Flight Dynamics | 14 |
| 3.1 Simulation Methods | 14 |
| 3.1.1 OpenRocket | 14 |
| 3.1.2 ZENITH | 14 |
| 3.2 Flight Profile | 15 |
| 3.3 Simulation Results | 15 |
| 3.3.1 Kinetic Energy Predictions | 15 |
| 3.3.2 Drift Predictions | 15 |
| 3.3.3 Descent Time Predictions | 15 |
| 3.4 Simulation Discrepancies | 15 |
| IV Payload | 16 |
| 4 Payload Sizing | 17 |
| 4.1 Sizing Algorithms | 17 |

| | |
|--------------------------------------------------|-----------|
| 5 Payload Deployment | 20 |
| 5.1 Requirements | 20 |
| 5.1.1 Top-level requirements | 20 |
| 5.1.2 Team-derived requirements | 22 |
| 5.2 Means of Securement | 22 |
| 5.3 Means of Deployment | 22 |
| 5.4 Leading Design | 22 |
| 6 Operational Protocols | 23 |
| 6.1 Transit & Deployment | 23 |
| 6.2 Descent | 24 |
| 6.3 Loiter | 24 |
| 6.4 Landing | 24 |
| 6.5 Retrieval | 24 |
| 7 Quadrotor Dynamic Model | 25 |
| 7.1 Coordinate Systems | 25 |
| 7.1.1 Coordinate Transformation | 26 |
| 7.2 Dynamic Model | 26 |
| 7.2.1 Nonlinear state space model | 28 |
| 7.2.2 Linearized state space model | 29 |
| 7.2.3 Discretization | 31 |
| 7.3 Simulation | 31 |
| 7.4 Controller Design | 32 |
| 7.4.1 LQR Tuning | 33 |
| V Safety | 35 |
| 8 Safety Plan Overview | 36 |
| 8.1 Emergency Preparedness | 36 |
| 8.2 Incident Reporting | 36 |
| 8.3 Equipment Training | 37 |
| 8.4 NAR/TRA Procedures | 37 |
| 9 Risk Assessment Overview | 39 |
| VI Project Plan | 40 |
| 10 Budget | 41 |
| 10.1 Structures and Recovery | 41 |
| Appendices | 42 |
| A NAR High-Power Rocketry Safety Code | 43 |
| B Federal Aviation Regulations 14 CFR 107 | 45 |
| C Federal Aviation Regulations 14 CFR 101 | 47 |

Bibliography**50**

Chapter 1

Preface

This document (ISS/USLI-PDR) serves as the [Preliminary Design Review \(PDR\)](#) for the University of Illinois at Urbana-Champaign University Student Launch Initiative team, [Illinois Space Society \(ISS\)](#). The content of this report will chiefly focus on the changes since the original proposal, developments in design and underlying justifications, as well as overall prospects and plans towards the [Critical Design Review \(CDR\)](#). In particular, the launch vehicle design is detailed with reference to the pertinent vehicle requirements, providing an overview of its subsystems, interfaces, and manufacturing methods. Safety considerations are addressed through a multitude of simulations, as well as a qualitative [Failure Modes and Effects Analysis \(FMEA\)](#) and [Environmental Impact Assessment \(EIA\)](#). Following this discussion, the payload requirements and preliminary design of both the airframe and sample retrieval mechanism are presented, culminating in the presentation of a detailed [Concept of Operations \(CONOPS\)](#). The payload-launch vehicle interface as well as the aerial deployment mechanism are discussed, giving rise to a detailed safety analysis. As part of the safety analysis, in addition to a comprehensive [FMEA](#), a [Personnel Hazard Analysis \(PHA\)](#) is presented. Any hazardous activities will be identified as part of this discussion, including any foreseeable contingencies and mitigation procedures. Finally, a project plan is presented, including a project timeline (Gantt chart), bill of materials, list of funding sources and mitigation procedures in case of delays.

This report is composed of six parts, in which each part builds forth upon the previous. These parts are:

- I Summary
- II Changes
- III Launch Vehicle
- IV Payload
- V Safety
- VI Project Plan

Each of these parts describes in due detail the developments and rationale behind the launch vehicle and payload design, as well as the overall implementation.

DISCLAIMER: While the authors have gone through great lengths to ensure the validity of all data presented in this document, all responsibility is assumed for any inconsistencies presented as part of this work.

Part I

Summary

Chapter 2

Executive Summary

Over the period spanning from proposal submission to [PDR](#) submission (August–November 2019), the team has made considerable progress in shaping a preliminary vehicle and payload design. Throughout these developments, the project chiefly guided by the the following main goals: safety, feasibility and timeliness. This part will outline the present mission design in relation to these goals, as well as the overall considerations that shaped the leading launch vehicle and payload design.

The launch vehicle is slated to be a single-booster rocket, weighing 10.68 kg (23.55 lbm), with a base-to-tip length of 2.41 m (7 ft 11 in). The vehicle caliber is two-fold, as a transition will be utilized so as to attain a wider fairing diameter; the body diameter is 10.16 cm (4 in), whereas the fairing, or payload bay, diameter is 15.24 cm (6 in). In designing the vehicle, a reference altitude of 1.5 km (4921 ft) was aimed at, prompting the appointment of the AeroTech K780R as the motor of choice. This motor has a burn time of 3 s, and produces a total impulse of 2371 N s (L-class). The nose cone was chosen to be of tangent ogive shape, with an aspect ratio of 3:1.

In reference to recovery of the vehicle, which forms a sizable portion of the mission's consideration in terms of both safety and system reusability, two parachutes are utilized; a 50.8 cm (20 in) diameter drogue parachute deployed at 800 ft, and a 183 cm (6 ft) diameter main parachute deployed at one second after apogee. Thus, the system will have a total of four segments: the booster (or lower) stage, the switchband, the upper stage, and the nose cone. Seeing as the [Unmanned Aerial Vehicle \(UAV\)](#) will not remain tethered nor lowered by parachute, it is not accounted for as a separate section. The final descent velocity of the vehicle is approximately 7 m s^{-1} , thereby satisfying the maximum terminal kinetic energy requirement.

In addition to the launch vehicle, a payload is necessary to effectuate the mission requirements, which state that a ground-based granular ice sample is to be retrieved and displaced by 10 ft (3.05 m). The present design is based on a [UAV](#) with four arms, each having one engine and rotor. The aforesighted payload bay allows for the payload to sit in the up right position with respect to the vehicle's descent attitude, such that upon deployment the system may immediately function as intended. To allow the [UAV](#) to descent unobstructed, the nose cone will be jettisoned by means of a high impulse carbon dioxide gas release, so as to force the nose cone parachute out. Upon jettison, this parachute will deploy and guide the nose cone down to a sufficiently low descent velocity. In transit, the [UAV](#) was secured in its stowed position using a solenoid-based mechanism. Lowering the payload requires a winch to unfurl after the solenoids have been disengaged, allow for the release of the payload which will slide out of the payload bay on four rails. Following these events, the [UAV](#) will be lowered using a winch system, after having released the This deployment will be commanded by way of a the rocket avionics system, which will command nose cone jettison

Part II

Changes

Part III

Launch Vehicle

Chapter 3

Flight Dynamics

The primary responsibility of the Flight Dynamics team is to simulate the performance of both the launch vehicle and the payload, to inform other subteams of constraints that must be satisfied to achieve safe flight, and to make design decisions on all structures and control systems that directly influence the flight of the launch vehicle-payload system.

3.1 Simulation Methods

In order to ensure that predictions of flight performance, as well as insights into possible design improvements, are robust and well-informed, the team is using two independent simulation programs to study the flight profile. The team is principally using OpenRocket for simulating the flight of the launch vehicle and predicting critical mission characteristics such as apogee, time to apogee, and total flight time, among many others. However, in addition to OpenRocket, the Flight Dynamics team is developing its own custom-built rocket simulation software, [Zenith Estimation through Numerical Integration and Tractable Heuristics \(ZENITH\)](#). The team considered using other open-source rocket-simulating software, but found that none of them were as sophisticated or accessible as OpenRocket, hence the team decided to develop its own program.

3.1.1 OpenRocket

OpenRocket is a powerful, open-source rocket flight simulation tool. As it is the most robust and informative, cost-free flight simulation tool available, the team is using it as the primary consultant on aerodynamic design considerations and predicting if the launch vehicle satisfies mission requirements. In addition to predicting flight trajectories, from launch to landing, for various possible initial conditions, OpenRocket also provides baseline estimates for the launch vehicle's mechanical and aerodynamic properties, including pre- and post-burnout masses, drag and lift coefficients, CP and CG locations, stability coefficient, and many others.

3.1.2 ZENITH

Due to a lack of satisfactory alternatives to OpenRocket, and in an attempt to gain a valuable learning experience in simulation design and implementation, the team elected to develop its own simulation of the launch vehicle. [ZENITH](#) is a Python-based program that simulates the trajectory of a high-power rocket with specified dimensions, mass and moments of inertia, and thrust curve, by numerically integrating a set of differential equations of motion that govern it. Aerodynamic coefficients are obtained from a database called AeroDB, which calculates such coefficients based on the provided dimensions of the rocket (IS THAT RIGHT????).

3.2 Flight Profile

The flight profile for this mission features a relatively simple sequence of events. Nominally at apogee of 4,700ft (and within 2 seconds after apogee), an ejection charge in the tube coupler will separate the upper and lower body tubes and deploy the drogue parachute as displayed in Figure 19. This will be the only explosive separation event of the entire flight. The main parachute will then deploy at 800ft (this is above the minimum parachute deployment altitude of 500ft). Within two seconds of main parachute deployment, the solenoid system in the fairing will trigger after the necessary RSO permission is acquired, priming the drone for deployment. The drone will then deploy passively by pushing the nose cone off and sliding downward from the rocket. The nose cone will not have a parachute. The process for jettisoning the nosecone is described in Sec. 4.2.2.5. The flight profile was simulated in OpenRocket using a model of the rocket with numerous design specifications (e.g. material and motor type) and simulated it with various initial conditions, such as wind speed, launch angle and direction, as well as the launch coordinates. As mentioned in the previous section, current projections show the rocket to satisfy all requirements of flight performance, thus validating the current flight profile. If necessary, the flight profile can be adjusted to better accommodate these requirements; for example, the altitude of main parachute deployment can be lowered to ensure that the drift distance remains within the recovery area.

3.3 Simulation Results

3.3.1 Kinetic Energy Predictions

3.3.2 Drift Predictions

3.3.3 Descent Time Predictions

3.4 Simulation Discrepancies

Part IV

Payload

Chapter 4

Payload Sizing

One of the core tenets of the payload design, lies in proper sizing of the **UAV** so as to ensure that the mission requirements are satisfied with due confidence. As such, an informed sizing methodology is required, few of which may be found in the literature pertaining to **Micro Air Vehicles (MAVs)**, the collective term for small **UAVs**. This chapter outlines the various algorithms considered, as well as the limitations and results obtained from the algorithm of choice. In this treatment, a brief overview of the state of the art is presented, followed by a number of implementational considerations pertaining to the algorithm of choice. Finally, sizing results are presented, which will be referred back to over the course of the remainder of this document.

4.1 Sizing Algorithms

In recent literature, the topic of **Micro Air Vehicle (MAV)** sizing has been treated at a number of occasions, but not to the extent of aircraft sizing. Bershadsky et al. [1] have developed the **Electric Multirotor Sizing Tool (EMST)**, an online **MAV** sizing algorithm. While this methodology seems very promising in its ability to accurately size **MAVs**, its implementation is not detailed in the aforementioned paper, and the online implementation has since been terminated.

A more recent approach has been presented by Winslow et al. [2], which shows excellent correlation with a set of reference **MAVs**. This approach rests on a series of parametric exponential equations that relate key inputs to component weight estimates as outputs. The approach presented in [2], as is the case in the sizing approach proposed by Shastry et al. [3], draws heavily on results from **Blade Element Momentum Theory (BEMT)**. This requires a degree of **Computational Fluid Dynamics (CFD)** to be implemented in the design loop, which was not regarded as a desirable property for the team's purposes. It was therefore sought to find tractable alternative that were less cumbersome in implementation, yet of higher fidelity. In particular, **BEMT** necessitates a two-dimensional **CFD** code to be ran so as to obtain planar aerodynamic coefficients. Subsequently, these coefficients are integrated over the complete blade lengths in an element-wise fashion (hence the name *blade element* momentum theory). A discussion regarding this decision follows below.

Aerodynamic data. A number of considerations have lead to the decision to employ manufacturer-provided experimental data, as opposed to either theoretical predictions or wind tunnel experiments. With reference to **CFD**-based approaches, given the abundance of standardized low-speed propeller geometries, as well as associated wind tunnel measurements, it is natural to opt for physical results, as they bear more fidelity. If **CFD** were to have been pursued, a number of simulation software packages would have substantially aided

in design, where XFLR5¹ and Q-Blade² would have been the prime contenders. These codes, having been produced for low speed aerodynamics and wind turbine blades, respectively, do not perform well for rotors with small cord length and high angular velocity. In the presence of high Reynolds numbers and localized supersonicity, both of which are observed in the rotors under consideration, the underlying aerodynamic models (in this case, the ISES model) fail, as they do not account for compressibility or trans-/supersonic effects [4].

Having discussed the drawbacks of computational methods, the two main experimental data sources can now be compared: wind tunnel data and motor-specific data. As for the first, there is a great wealth of low speed aerodynamic wind tunnel data that has been acquired as part of the work of Prof. Selig's group at the University of Illinois [5]. This database provides high-fidelity aerodynamic coefficients for a wide variety of standardized propeller geometries, at different flow conditions and orientations. For these reasons, it would appear to be an excellent source of data for the purpose of sizing the UAV. However, to properly determine the required power system sizing and engines of choice, it is necessary to include existing motor-propeller combinations in the sizing algorithm. This mainly stems from the fact that different torques and levels of power consumption are experienced depending on both the motor and rotor choice, thereby necessitating either an implicit assumption regarding motor efficiency, or the use of existing empirical data supplied by manufacturers. In the interest of attaining a high-fidelity code, it was deemed more appropriate to utilize test data provided by manufacturers, and augment this as needed by means of the data from [5]. Having made this decision, it is now of importance to compile a list of reference motors for use in the subsequent trade-off study and optimization effort.

Reference motor selection. As mentioned before, a number of motors is to be selected for use in the sizing algorithm based on the methodology of Winslow et al. [2]. In an attempt to maintain homogeneity of the test setup and data format across the various types of motors, it was quickly realized that selecting a single vendor would insure data integrity and equivalence to a greater degree, as opposed to mixing data. As such, SunnySky USA³ was chosen as the prime vendor, given the quality of their test data and general data sheets, as well as past experience with the company. The following engines and propeller considerations have been implemented as part of the framework adapted from Winslow et al. [2]:

¹<http://www.xflr5.tech/xflr5.htm>

²<http://q-blade.org/>

³<https://sunnyskyusa.com/>

| Motor | Speed constant (K_b) | Propeller | Voltage |
|--------------------------|------------------------------------------|---------------------------------------------|----------------|
| <i>SunnySky X2302 V3</i> | 1500/1650 | GWS8043, GWS8060, GWS9050 | 7.4/8.4 |
| | 1400 | GWS8043, GWS8060, GWS9050, GWS1047 | 7.4/8.4 |
| <i>SunnySky X2304 V3</i> | 1480 | GWS8043, GWS8060, GWS9047, GWS9050 | 7.4/8.4 |
| | 1800 | GWS8043, GWS8060, GWS9047, GWS9050 | 7.4/8.4 |
| <i>SunnySky X2212 V3</i> | 980 | APC9045, APC9047, APC1038, APC1047 | 11.1 |
| | | APC8038, APC9045, APC9047, APC1047 | 14.8 |
| <i>SunnySky X2212 V3</i> | 1250 | APC8060, APC9045, APC9047, APC9060 | 11.1 |
| | | APC8060 | 14.8 |
| <i>SunnySky X2216 V3</i> | 1400 | APC7060, APC8038, APC8060, APC9045, APC9047 | 11.1 |
| | | APC7060 | 14.8 |
| <i>SunnySky X2216 V3</i> | 880 | APC9045, APC1047, APC1147 | 11.1 |
| | | APC8038, APC9045, APC9060, APC1047 | 14.8 |
| <i>SunnySky X2216 V3</i> | 950 | APC9045, APC1047, APC1147 | 11.1 |
| | | APC9045, APC9060, APC1047 | 14.8 |
| <i>SunnySky X2216 V3</i> | 1100 | APC9045, APC9047, APC9060, APC1047, APC1147 | 11.1 |
| | | APC8060, APC9045, APC9047, APC9060 | 14.8 |
| <i>SunnySky X2216 V3</i> | 1250 | APC9045, APC9047, APC9060, APC1047, APC1147 | 11.1 |
| | | APC8060 | 14.8 |
| <i>SunnySky X2216 V3</i> | 1400 | APC8060, APC9045, APC9047, APC9060 | 11.1 |
| | | APC7060, APC8060 | 14.8 |

Chapter 5

Payload Deployment

During the boost, coast, and the majority of the launch vehicle's flight, the payload will remain idle and securely fixed in the payload bay. This chapter will detail the means of securement and deployment of the payload, as well as a trade-off between the various means that have been considered to arrive at the leading design.

This chapter will be structured as follows: Sec. 5.1 details the requirements the payload is to satisfy given the overall mission and top-level requirements, followed by a trade-off study regarding the means of securement in Sec. 5.2, as well as the possible deployment modes in Sec. 5.3. Finally, the leading design is presented in Sec. 5.4 in reference to the foregoing trade-off studies.

5.1 Requirements

This section details the various requirements to which the payload deployment scheme must abide. Specifically, two forms of requirements are identified: top-level requirements and team-derived requirements. The first are requirements either imposed by the competition, or legislation that is in effect at the time of launch and operations. The second form of requirements pertain to what the team perceives to be of importance in assuring mission success and robustness.

5.1.1 Top-level requirements

The top-level requirements for the payload deployment are outlined in Secs. 4.3–4 of [6], reading as follows:

4.4. Lunar Ice Sample Recovery Mission Requirements

- 4.3.1. Teams must abide by all [Federal Aviation Authority \(FAA\)](#) and [National Association of Rocketry \(NAR\)](#) rules and regulations.
- 4.3.2. Black Powder and/or similar energetics are only permitted for deployment of in-flight recovery systems. Any ground deployments must utilize mechanical systems.
- 4.3.3. Any part of the payload or vehicle that is designed to be deployed, whether on the ground or in the air, must be fully retained until it is deployed as designed.
 - 4.3.7.1. A mechanical retention system will be designed to prohibit premature deployment.
 - 4.3.7.2. The retention system will be robust enough to successfully endure flight forces experienced during both typical and atypical flights.
 - 4.3.7.3. The designed system will be fail-safe.
 - 4.3.7.4. Exclusive use of shear pins will not meet this requirement.

4.6. Special Requirements for UAVs and Jettisoned Payloads

- 4.4.1. Any experiment element that is jettisoned during the recovery phase will receive real-time Range Safety Officer (RSO) permission prior to initiating the jettison event.
 - 4.4.2. UAV payloads, if designed to be deployed during descent, will be tethered to the vehicle with a remotely controlled release mechanism until the RSO has given permission to release the UAV.
 - 4.4.3. Teams flying UAVs will abide by all applicable FAA regulations, including the FAA's Special Rule for Model Aircraft (Public Law 112-95 Section 336; see <https://www.faa.gov/uas/faqs>).
 - 4.4.4. Any UAV weighing more than .55 lbs. will be registered with the FAA and the registration number marked on the vehicle.

In addition, by [FAA](#) regulations [7], the [UAV](#) may only be operated below 400 ft in [Line of Sight \(LOS\)](#)¹. From the [FAA Reauthorization Act of 2018](#), the following pertinent regulations may be found. The [UAV](#) must have a gross weight under 4.4 lbm, and must be operated:

- (i) within or beyond visual LOS of the operator;
 - (ii) less than 400 ft above ground;
 - (iii) during daylight conditions;
 - (iv) within Class G airspace; and
 - (v) outside of 5 statute miles from any airport, heliport, seaplane base, spaceport, or other location with aviation activities.

As a supplement to these regulations, an aeronautical chart of the surroundings of the launch site (Bragg Farms, Hazel Green, AL) is given in Fig. 5.1.

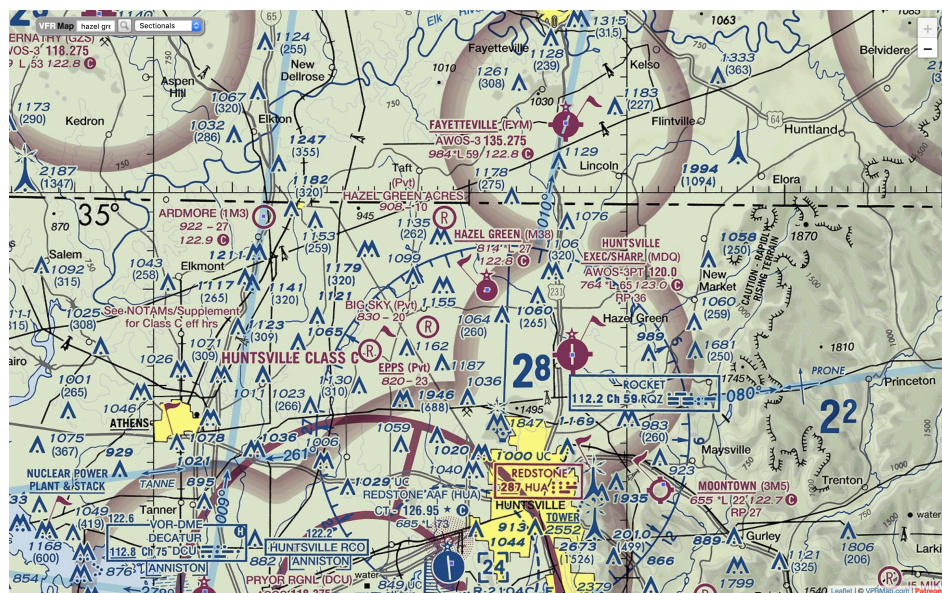


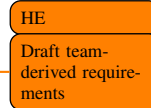
Figure 5.1: Visual Flight Rules (VFR) aeronautical chart of the Hazel Green, AL area. Adapted from [VFRMap.com](#)

¹FAA Reauthorization Act of 2018 §346(b.2.C), 49 U.S.C. §44806

In this chart, the Class E airspace is bounded by a vignette magenta border, and spans down to 700 ft; anything below that is Class G airspace, and thus open for [UAV](#) operations. Incidentally, the area of payload operations lies beyond a 5 mile radius of the closest airfield.

5.1.2 Team-derived requirements

In addition to the above, a number of additional requirements have been compiled by the team. In particular, the robustness of the securement system, as well as the reliability of the deployment system are at the center of the discussion.



5.2 Means of Securement

5.3 Means of Deployment

5.4 Leading Design

Chapter 6

Operational Protocols

Throughout the mission, the **UAV** will encounter a number of varied tasks that must be completed sequentially so as to satisfy the mission objectives. As such, it is natural to define a number of regimes in which the vehicle must operate, as these dictate the operational protocols that are to be effectuated. This chapter details these operational regimes, including the pertinent operational protocols. Specifically, the following regimes are identified and discussed in due detail:

- I. Transit & Deployment
- II. Descent
- III. Loiter
- IV. Landing
- V. Retrieval

6.1 Transit & Deployment

Throughout stand-by, launch and passive descent, referred to as 'transit', the **UAV** will assume a low-power mode, periodically sending status updates and seeking connection with a ground station. This passive mode stems from multiple considerations. First, given the limited power supply, as much power as possible is to be saved will still maintaining a connection with the **UAV**. Second, by **FAA** regulations, the **UAV** may only be operated below 400 ft in **LOS**¹ [7]. To ensure that no active operation takes place above this ceiling, the vehicle will restrict its operations by considering its current altimeter reading as a locking mechanism. This 'altitude lock' constitutes the transit phase.

From the **FAA Reauthorization Act of 2018**, the following pertinent regulations may be found. The **UAV** must have a gross weight under 4.4 lbm, and must be operated:

- (i) within or beyond visual **LOS** of the operator;
- (ii) less than 400 ft above ground;
- (iii) during daylight conditions;
- (iv) within Class G airspace; and
- (v) outside of 5 statute miles from any airport, heliport, seaplane base, spaceport, or other location with aviation activities.

¹FAA Reauthorization Act of 2018 §346(b.2.C), 49 U.S.C. §44806

Regarding points (iv) and (v), it is found that the closest airport is the Hazel Green airport. However, the launch site, Bragg Farms, is located outside of the Class E airspace, thus respecting the Class G airspace requirement.

Given the fact that the payload will only be deployed upon being granted permission from the **RSO**, it is of importance to achieve a timely response in the event of late notification. In addition, proper coordination with the avionics systems is of importance, as solenoid disengagement and winch lowering must be followed by **UAV** arm deployment in close succession.

6.2 Descent

Given the limited time of flight the **UAV** is capable of achieving, it is of importance to conclude the descent phase in as small of a time frame as possible.

HE
Expand on deployment requirements (robustness, rapidity) and ground proximity considerations

6.3 Loiter

HE
Expand on descent phase, including trade-offs between guidance algorithms ((N)MPC, GPC) and waypoint tracking vs. visual guidance at close proximity (CV).

6.4 Landing

HE
Expand on loiter phase, highlighting energy efficiency and data acquisition (feature detection and path planning) during idle phase. Also detail what safety features must be incorporated into this phase (geofencing, no-fly zones have to default back to loiter).

6.5 Retrieval

HE
Expand on final approach and landing phase, including close-quarters operations and the role of computer vision in detecting the landing site, as well as the accuracy and terminal touch down conditions (velocity, attitude). Explain touch-and-go maneuvers in case of failed landing attempt.

HE
Expand on retrieval protocol, including claw operations and validation of claw contents. Explain the details on distancing and claw placement.

Chapter 7

Quadrotor Dynamic Model

7.1 Coordinate Systems

Let us consider the following four coordinate systems: (i) inertial, (ii) Earth-fixed, (iii) instantaneous topocentric, and (iv) body-fixed [8, pp. 3f.]. For these systems, the axes are defined as follows:

Inertial system (O at Earth center)

- X** On the Earth equatorial plane, pointing to the zero longitude at take-off
- Y** On the Earth equatorial plane, pointing to the 90° longitude at take-off
- Z** Perpendicular to the equatorial plane, pointing to the North Pole

Earth-fixed system (O_E at Earth center)

- X_E** On the Earth equatorial plane, always pointing to the Greenwich (0°) longitude
- Y_E** On the Earth equatorial plane, always pointing to the 90° longitude
- Z_E** Perpendicular to the equatorial plane, pointing to the North Pole

Instantaneous topocentric system (O_T at the projection point of the moving UAV on the Earth surface)

- x_T** On the local horizon plane tangent to the instantaneous projection point of the UAV, directed along the local geocentric North
- y_T** On the local horizon plane tangent to the instantaneous projection point of the UAV, directed along the local geocentric North
- z_T** Perpendicular to the instantaneous tangent plane, directed along the geocentric radius vector and pointing toward the Earth center

Body-fixed system (O_B at the center of gravity of the UAV)

- x_B** Along the UAV principle (longitudinal) axis, positive forward
- y_B** Normal to the x_B - z_B symmetric plane, completing the right-hand system
- z_B** In the principle plane of symmetry of the UAV, perpendicular to the x_B axis and positive downward

We will chiefly confine our discussion to the O_T (instantaneous topocentric system) and O_B (body-fixed) frames, as the distances the vehicle will travel allow for a flat Earth approximation with constant uniform gravity [9]. Let us now consider the coordinate transformation between these two frames:

7.1.1 Coordinate Transformation

Let us define the following Euler angles:

- θ Pitch
- ψ Yaw
- ϕ Roll

We then find the transformation from the instantaneous topocentric frame to the body-centric frame to be [10, Eq. 2-2]:

$$\begin{aligned} [R]_{T \rightarrow B}(\theta, \psi, \phi) &= \begin{bmatrix} 1 & 0 & 0 \\ 0 & \cos \phi & \sin \phi \\ 0 & -\sin \phi & \cos \phi \end{bmatrix} \begin{bmatrix} \cos \theta & 0 & -\sin \theta \\ 0 & 1 & 0 \\ \sin \theta & 0 & \cos \theta \end{bmatrix} \begin{bmatrix} \cos \psi & \sin \psi & 0 \\ -\sin \psi & \cos \psi & 0 \\ 0 & 0 & 1 \end{bmatrix} \\ &= \begin{bmatrix} \cos \theta \cos \psi & \cos \theta \sin \psi & -\sin \theta \\ \sin \theta \cos \psi \sin \phi - \sin \psi \cos \phi & \sin \theta \sin \psi \sin \phi + \cos \psi \cos \phi & \cos \theta \sin \phi \\ \sin \theta \cos \psi \cos \phi + \sin \psi \sin \phi & \sin \theta \sin \psi \cos \phi - \cos \psi \sin \phi & \cos \theta \cos \phi \end{bmatrix} \quad (7.1.1) \end{aligned}$$

Given the nature of the transformation matrix, it is readily found that:

$$[R]_{B \rightarrow T} = [R]_{T \rightarrow B}^{-1} = [R]_{T \rightarrow B}^T \quad (7.1.2)$$

7.2 Dynamic Model

Given the complex nature of the rotor-based UAV, we will make the following a priori assumptions to aid in the derivation of the vehicle model:

1. The UAV is a rigid body.
2. The Tensor of Inertia (ToI) of the UAV is approximated as the Moment of Inertia (MoI) of several objects.
3. The Center of Mass (CM) coincides with the UAV's geometrical centroid.
4. The MoI of the propellers is neglected.
5. Time delay of commands is neglected.
6. Aerodynamic drag force is neglected.

While most of the aforestated simplifications are intuitively sound, neglecting the aerodynamic drag force begs for justification. Castillo et al. [11] provide the following approximation to the UAV drag force:

$$\mathbf{f}_{d_k} = C_{D_k} \rho A_k V_k (V_{w_k} - V_k) \hat{\mathbf{k}}, \quad k : x_b, y_b, z_b \quad (7.2.1)$$

Where $\hat{\mathbf{k}}$ is the unit vector in \mathbf{k} direction, A_k is the reference area by which the drag coefficient C_{D_k} is determined in the \mathbf{k} -direction. V_k and V_{w_k} are the vehicle velocity and wind velocity in O_B , respectively, and ρ is the air density, which is assumed to be constant. In this formulation, C_{D_k} is to be determined

through simulation ([CFD](#)) or experiment. However, this poses a significant difficulty: the [UAV](#) consists of many distinct components with orientation and speed dependent drag characteristics, making the definition of a constant C_{D_k} inadvisable. As a matter of fact, Castillo et al. [11] treat the drag force as an unknown disturbance that is to be counteracted by the control system, thus warranting the term to be dropped.

Let us define \mathbf{T} and \mathbf{H} , the thrust force and hub torque for every motor–propeller system, respectively. Research shows that these forces scale with the square of the angular rate of the propellor [1, 2, 10–12], i.e.:

$$T_i = k_T \omega_i^2 \quad (7.2.2)$$

$$H_i = k_H \omega_i^2 \quad (7.2.3)$$

where i denotes the i 'th propeller, and we assume the propellers to be identical, yielding constant k_T, k_H . These coefficients can be found experimentally. Following the Newton–Euler approach presented by Kurak and Hodzic [10], we find for a symmetric four-propeller [UAV](#) layout:

$$\ddot{\phi} = \frac{\ell(T_2 - T_4) - (I_z - I_y)\dot{\theta}\dot{\psi}}{I_x} \quad (7.2.4)$$

$$\ddot{\theta} = \frac{\ell(T_3 - T_1) - (I_x - I_z)\dot{\phi}\dot{\psi}}{I_y} \quad (7.2.5)$$

$$\ddot{\psi} = \frac{(H_1 + H_3) - (H_2 + H_4) - (I_y - I_x)\dot{\phi}\dot{\theta}}{I_z} \quad (7.2.6)$$

$$\ddot{x} = \frac{(\cos \phi \sin \theta \cos \psi + \sin \phi \sin \psi) \sum_{i=1}^4 T_i}{m} \quad (7.2.7)$$

$$\ddot{y} = \frac{(\cos \phi \sin \theta \sin \psi - \sin \phi \cos \psi) \sum_{i=1}^4 T_i}{m} \quad (7.2.8)$$

$$\ddot{z} = \frac{(\cos \phi \cos \theta) \sum_{i=1}^4 T_i - mg}{m} \quad (7.2.9)$$

where $I_k = I_{kk}, k : x, y, z$ are the diagonal elements of the [ToI](#) \mathbf{I} , ℓ is the L_2 -distance between the propeller and the origin of the O_B -frame (ℓ is constant to satisfy symmetry).

7.2.1 Nonlinear state space model

Let us define the following state variable:

$$\mathbf{x} = \begin{bmatrix} \phi \\ \dot{\phi} \\ \theta \\ \dot{\theta} \\ \psi \\ \dot{\psi} \\ z \\ \dot{z} \\ x \\ \dot{x} \\ y \\ \dot{y} \end{bmatrix} = \begin{bmatrix} x_1 \\ x_2 = \dot{x}_1 \\ x_3 \\ x_4 = \dot{x}_3 \\ x_5 \\ x_6 = \dot{x}_5 \\ x_7 \\ x_8 = \dot{x}_7 \\ x_9 \\ x_{10} = \dot{x}_9 \\ x_{11} \\ x_{12} = \dot{x}_{11} \end{bmatrix} \quad (7.2.10)$$

The force control input is then defined as:

$$\mathbf{u}^* = \begin{bmatrix} \sum_{i=1}^4 T_i \\ T_2 - T_4 \\ T_3 - T_1 \\ (H_1 + H_3) - (H_2 + H_4) \end{bmatrix} \quad (7.2.11)$$

Defining the angular rate control input as:

$$\mathbf{u} = \begin{bmatrix} \omega_1^2 \\ \omega_2^2 \\ \omega_3^2 \\ \omega_4^2 \end{bmatrix} \quad (7.2.12)$$

Using this definition, we find the force control input \mathbf{u}^* to be related to the angular rate control input \mathbf{u} as follows:

$$\mathbf{u}^* = \begin{bmatrix} k_T & k_T & k_T & k_T \\ 0 & k_T & 0 & -k_T \\ -k_T & 0 & k_T & 0 \\ k_H & -k_H & k_H & -k_H \end{bmatrix} \mathbf{u} \quad (7.2.13)$$

Let us now define the following constants:

$$a_1 = \frac{I_y - I_z}{I_x} \quad a_2 = \frac{I_z - I_x}{I_y} \quad a_3 = \frac{I_x - I_y}{I_z} \quad (7.2.14)$$

$$b_1 = \frac{\ell}{I_x} \quad b_2 = \frac{\ell}{I_y} \quad b_3 = \frac{\ell}{I_3} \quad (7.2.15)$$

and the following rotations:

$$\begin{aligned} r_t &= \cos \phi \cos \theta \\ r_x &= \cos \phi \sin \theta \cos \psi + \sin \phi \sin \psi \\ r_y &= \cos \phi \sin \theta \sin \psi - \sin \phi \cos \psi \end{aligned} \quad (7.2.16)$$

The nonlinear state space formulation is then found to be:

$$\dot{\mathbf{x}} = \begin{bmatrix} x_2 \\ x_4 x_6 a_1 + b_1 u_2^* \\ x_4 \\ x_2 x_6 a_2 + b_2 u_3^* \\ x_6 \\ x_2 x_4 a_3 + b_3 u_4^* \\ x_8 \\ -g + r_t(x_1, x_3) u_1^* / m \\ x_{10} \\ r_x(x_1, x_3, x_5) u_1^* / m \\ x_{12} \\ r_y(x_1, x_3, x_5) u_1^* / m \end{bmatrix} \quad (7.2.17)$$

7.2.2 Linearized state space model

Let us apply a small angle approximation on Eq. 7.2.16, giving:

$$\begin{aligned} r_t &\approx 1 \\ r_x &\approx \theta \\ r_y &\approx \theta\psi - \phi \approx -\phi \end{aligned} \quad (7.2.18)$$

To linearize Eq. 7.2.17, we must find a suitable equilibrium point, where $\dot{\mathbf{x}} = \mathbf{0}$. This holds for:

$$\begin{aligned} \bar{\mathbf{x}} &= \begin{bmatrix} 0 & 0 & 0 & 0 & 0 & 0 & \bar{x}_7 & 0 & \bar{x}_9 & 0 & \bar{x}_{11} \end{bmatrix}^\top \\ \bar{\mathbf{u}}^* &= \begin{bmatrix} mg & 0 & 0 & 0 \end{bmatrix}^\top \end{aligned} \quad (7.2.19)$$

Linearizing Eq. 7.2.17 about $(\bar{\mathbf{x}}, \bar{\mathbf{u}}^*)$, we obtain:

$$\begin{aligned} \mathbf{A} &= \left. \frac{\partial \dot{\mathbf{x}}(\mathbf{x}, \mathbf{u}^*)}{\partial \mathbf{x}} \right|_{(\bar{\mathbf{x}}, \bar{\mathbf{u}}^*)} \\ \mathbf{B} &= \left. \frac{\partial \dot{\mathbf{x}}(\mathbf{x}, \mathbf{u}^*)}{\partial \mathbf{u}^*} \right|_{(\bar{\mathbf{x}}, \bar{\mathbf{u}}^*)} \end{aligned} \quad (7.2.20)$$

which yields the following state space formulation:

$$\begin{aligned}
 \dot{\mathbf{x}} &= \underbrace{\begin{bmatrix} 0 & 1 & 0 & 0 & 0 & 0 & 0 & 0 & 0 & 0 & 0 & 0 \\ 0 & 0 & 0 & 0 & 0 & 0 & 0 & 0 & 0 & 0 & 0 & 0 \\ 0 & 0 & 0 & 1 & 0 & 0 & 0 & 0 & 0 & 0 & 0 & 0 \\ 0 & 0 & 0 & 0 & 0 & 0 & 0 & 0 & 0 & 0 & 0 & 0 \\ 0 & 0 & 0 & 0 & 0 & 0 & 1 & 0 & 0 & 0 & 0 & 0 \\ 0 & 0 & 0 & 0 & 0 & 0 & 0 & 0 & 0 & 0 & 0 & 0 \\ 0 & 0 & 0 & 0 & 0 & 0 & 0 & 0 & 0 & 0 & 0 & 0 \\ 0 & 0 & 0 & 0 & 0 & 0 & 0 & 1 & 0 & 0 & 0 & 0 \\ 0 & 0 & 0 & 0 & 0 & 0 & 0 & 0 & 0 & 0 & 0 & 0 \\ 0 & 0 & 0 & 0 & 0 & 0 & 0 & 0 & 0 & 0 & 1 & 0 \\ 0 & g & 0 & 0 & 0 & 0 & 0 & 0 & 0 & 0 & 0 & 0 \\ -g & 0 & 0 & 0 & 0 & 0 & 0 & 0 & 0 & 0 & 0 & 0 \end{bmatrix}}_{\mathbf{A}} \mathbf{x} + \underbrace{\begin{bmatrix} 0 & 0 & 0 & 0 \\ 0 & b_1 & 0 & 0 \\ 0 & 0 & 0 & 0 \\ 0 & 0 & b_2 & 0 \\ 0 & 0 & 0 & 0 \\ 0 & 0 & 0 & b_3 \\ 0 & 0 & 0 & 0 \\ 1/m & 0 & 0 & 0 \\ 0 & 0 & 0 & 0 \\ 0 & 0 & 0 & 0 \\ 0 & 0 & 0 & 0 \\ 0 & 0 & 0 & 0 \end{bmatrix}}_{\mathbf{B}^*} \mathbf{u}^* \\
 &= \mathbf{Ax} + \underbrace{\begin{bmatrix} 0 & 0 & 0 & 0 \\ 0 & b_1 k_T & 0 & -b_1 k_T \\ 0 & 0 & 0 & 0 \\ -b_2 k_T & 0 & b_2 k_T & 0 \\ 0 & 0 & 0 & 0 \\ b_3 k_H & -b_3 k_H & b_3 k_H & -b_3 k_H \\ 0 & 0 & 0 & 0 \\ \frac{k_T}{m} & \frac{k_T}{m} & \frac{k_T}{m} & \frac{k_T}{m} \\ 0 & 0 & 0 & 0 \\ 0 & 0 & 0 & 0 \\ 0 & 0 & 0 & 0 \end{bmatrix}}_{\mathbf{B}} \mathbf{u}
 \end{aligned} \tag{7.2.21}$$

7.2.3 Discretization

Zero-order Hold (ZOH) discretization of Eq. 7.2.21, gives for constant sampling time h :

$$\Phi = e^{Ah} = \begin{bmatrix} 1 & h & 0 & 0 & 0 & 0 & 0 & 0 & 0 & 0 & 0 & 0 \\ 0 & 1 & 0 & 0 & 0 & 0 & 0 & 0 & 0 & 0 & 0 & 0 \\ 0 & 0 & 1 & h & 0 & 0 & 0 & 0 & 0 & 0 & 0 & 0 \\ 0 & 0 & 0 & 1 & 0 & 0 & 0 & 0 & 0 & 0 & 0 & 0 \\ 0 & 0 & 0 & 0 & 1 & h & 0 & 0 & 0 & 0 & 0 & 0 \\ 0 & 0 & 0 & 0 & 0 & 1 & h & 0 & 0 & 0 & 0 & 0 \\ 0 & 0 & 0 & 0 & 0 & 0 & 1 & 0 & 0 & 0 & 0 & 0 \\ 0 & 0 & 0 & 0 & 0 & 0 & 0 & 1 & h & 0 & 0 & 0 \\ 0 & \frac{gh^2}{2} & 0 & 0 & 0 & 0 & 0 & 0 & 1 & h & 0 & 0 \\ 0 & gh & 0 & 0 & 0 & 0 & 0 & 0 & 0 & 1 & 0 & 0 \\ -\frac{gh^2}{2} & -\frac{gh^3}{6} & 0 & 0 & 0 & 0 & 0 & 0 & 0 & 0 & 1 & h \\ -gh & -\frac{gh^2}{2} & 0 & 0 & 0 & 0 & 0 & 0 & 0 & 0 & 0 & 1 \end{bmatrix} \quad (7.2.22)$$

$$\Gamma = \int_0^h e^{As} ds \cdot \mathbf{B} = \begin{bmatrix} 0 & \frac{1}{2}b_1h^2k_T & 0 & -\frac{1}{2}b_1h^2k_T \\ 0 & b_1hk_T & 0 & b_1(-h)k_T \\ -\frac{1}{2}b_2h^2k_T & 0 & \frac{1}{2}b_2h^2k_T & 0 \\ b_2(-h)k_T & 0 & b_2hk_T & 0 \\ \frac{1}{2}b_3h^2k_H & -\frac{1}{2}b_3h^2k_H & \frac{1}{2}b_3h^2k_H & -\frac{1}{2}b_3h^2k_H \\ b_3hk_H & b_3(-h)k_H & b_3hk_H & b_3(-h)k_H \\ \frac{h^2k_T}{h^2k_T} & \frac{h^2k_T}{h^2k_T} & \frac{h^2k_T}{h^2k_T} & \frac{h^2k_T}{h^2k_T} \\ \frac{h^2k_T}{h^2k_T} & \frac{h^2k_T}{h^2k_T} & \frac{h^2k_T}{h^2k_T} & \frac{h^2k_T}{h^2k_T} \\ 0 & \frac{1}{6}b_1gh^3k_T & 0 & -\frac{1}{6}b_1gh^3k_T \\ 0 & \frac{1}{2}b_1gh^2k_T & 0 & -\frac{1}{2}b_1gh^2k_T \\ 0 & -\frac{1}{24}b_1gh^4k_T & 0 & \frac{1}{24}b_1gh^4k_T \\ 0 & -\frac{1}{6}b_1gh^3k_T & 0 & \frac{1}{6}b_1gh^3k_T \end{bmatrix} \quad (7.2.22)$$

with the following state space system:

$$\mathbf{x}(k+1) = \Phi\mathbf{x}(k) + \Gamma\mathbf{u}(k) \quad (7.2.23)$$

7.3 Simulation

From Tayebi and McGilvray [13], we adopt the following values for our simulation:

Table 7.1: Simulation parameters [13]

| Parameter | Value |
|-----------|------------------------------------------------------------|
| g | 9.81 m s^{-2} |
| m | 0.468 kg |
| ℓ | 0.225 m |
| k_T | $2.980 \times 10^{-6} (\text{rad}^2/\text{s}^2)/\text{N}$ |
| k_H | $1.140 \times 10^{-7} (\text{rad}^2/\text{s}^2)/\text{Nm}$ |
| I_x | $4.856 \times 10^{-3} \text{ kg m}^{-2}$ |
| I_y | $4.856 \times 10^{-3} \text{ kg m}^{-2}$ |
| I_z | $8.801 \times 10^{-3} \text{ kg m}^{-2}$ |

Letting $h = 1 \times 10^{-3} \text{ s}$, we obtain:

$$\Phi = \begin{bmatrix} 1 & 0.001 & 0 & 0 & 0 & 0 & 0 & 0 & 0 & 0 & 0 \\ 0 & 1 & 0 & 0 & 0 & 0 & 0 & 0 & 0 & 0 & 0 \\ 0 & 0 & 1 & 0.001 & 0 & 0 & 0 & 0 & 0 & 0 & 0 \\ 0 & 0 & 0 & 1 & 0 & 0 & 0 & 0 & 0 & 0 & 0 \\ 0 & 0 & 0 & 0 & 1 & 0.001 & 0 & 0 & 0 & 0 & 0 \\ 0 & 0 & 0 & 0 & 0 & 1 & 0 & 0 & 0 & 0 & 0 \\ 0 & 0 & 0 & 0 & 0 & 0 & 1 & 0.001 & 0 & 0 & 0 \\ 0 & 0 & 0 & 0 & 0 & 0 & 0 & 1 & 0 & 0 & 0 \\ 0 & 4.905 \times 10^{-6} & 0 & 0 & 0 & 0 & 0 & 0 & 1 & 0.001 & 0 \\ 0 & 0.00981 & 0 & 0 & 0 & 0 & 0 & 0 & 0 & 1 & 0 \\ -4.905 \times 10^{-6} & -1.635 \times 10^{-9} & 0 & 0 & 0 & 0 & 0 & 0 & 0 & 0 & 1 \\ -0.00981 & -4.905 \times 10^{-6} & 0 & 0 & 0 & 0 & 0 & 0 & 0 & 0 & 1 \end{bmatrix} \quad (7.3.1)$$

$$\Gamma = \begin{bmatrix} 1 & 0.001 & 0 & 0 & 0 & 0 & 0 & 0 & 0 & 0 & 0 \\ 0 & 1 & 0 & 0 & 0 & 0 & 0 & 0 & 0 & 0 & 0 \\ 0 & 0 & 1 & 0.001 & 0 & 0 & 0 & 0 & 0 & 0 & 0 \\ 0 & 0 & 0 & 1 & 0 & 0 & 0 & 0 & 0 & 0 & 0 \\ 0 & 0 & 0 & 0 & 1 & 0.001 & 0 & 0 & 0 & 0 & 0 \\ 0 & 0 & 0 & 0 & 0 & 1 & 0 & 0 & 0 & 0 & 0 \\ 0 & 0 & 0 & 0 & 0 & 0 & 1 & 0.001 & 0 & 0 & 0 \\ 0 & 4.905 \times 10^{-6} & 0 & 0 & 0 & 0 & 0 & 0 & 1 & 0.001 & 0 \\ 0 & 0.00981 & 0 & 0 & 0 & 0 & 0 & 0 & 0 & 1 & 0 \\ -4.905 \times 10^{-6} & -1.635 \times 10^{-9} & 0 & 0 & 0 & 0 & 0 & 0 & 0 & 0 & 1 \\ -0.00981 & -4.905 \times 10^{-6} & 0 & 0 & 0 & 0 & 0 & 0 & 0 & 0 & 1 \end{bmatrix}$$

7.4 Controller Design

This section details the controller setup and design for the UAV. We concern ourselves chiefly with the servo problem, with path generation being delegated to the guidance law. Given the nature of the problem, we are

forced to employ the [LQR](#) methodology to tune the gains for this [Multiple Input Multiple Output \(MIMO\)](#) system.

7.4.1 LQR Tuning

Following the guidelines from [14], we are to work with the following cost function:

$$\mathcal{J} = \rho \mathbf{x}^\top \mathbf{H}_w^\top \bar{\mathbf{Q}}_1 \mathbf{H}_w \mathbf{x} + \mathbf{u}^\top \mathbf{Q}_2 \mathbf{u} \quad (7.4.1)$$

where \mathbf{Q} is a diagonal matrix containing elements that equal the inverse of the square of the maximum deviation of the states/inputs of interest. The value of ρ is to be tuned by trial and error, considering the properties of the response.

State weighting matrix. Since we wish to have full state control with minimal deviations on every state, we will pose $\mathbf{H}_w = \mathbf{I}_{12}$. Given this choice of \mathbf{H}_w , we find $\bar{\mathbf{Q}}_1 = \mathbf{Q}_1$. We find $\bar{\mathbf{Q}}_1$ to be of the form:

$$\bar{\mathbf{Q}}_1 = \begin{bmatrix} \Delta x_1^{-2} & 0 & \dots & 0 \\ 0 & \Delta x_2^{-2} & \ddots & \vdots \\ \vdots & \ddots & \ddots & 0 \\ 0 & \dots & 0 & \Delta x_{12}^{-2} \end{bmatrix} \quad (7.4.2)$$

where the entries are tabulated in Tab. 7.2. The rationale behind the magnitude of these bounds lies in the mission objective of the [UAV](#); we wish to accomplish minute maneuvering and near-stationary hovering with closely matching attitude and small slew rate. As can be seen from the values, we place a greater importance on the vertical (z -axis) motion, such that the vehicle can accomplish accurate terrain following and close-quarters operations close to the surface.

Table 7.2: Maximum state deviation values for use in the $\bar{\mathbf{Q}}_1$ matrix in the [LQR](#) routine

| State | Variable | Maximum state deviation |
|-----------------|----------------|----------------------------------------------------------------------------|
| Δx_1 | ϕ | $2.5^\circ \approx 4.36 \times 10^{-2} \text{ rad}$ |
| Δx_2 | $\dot{\phi}$ | $1.25^\circ \text{ s}^{-1} \approx 2.18 \times 10^{-2} \text{ rad s}^{-1}$ |
| Δx_3 | θ | $2.5^\circ \approx 4.36 \times 10^{-2} \text{ rad}$ |
| Δx_4 | $\dot{\theta}$ | $1.25^\circ \text{ s}^{-1} \approx 2.18 \times 10^{-2} \text{ rad s}^{-1}$ |
| Δx_5 | ψ | $5^\circ \approx 8.73 \times 10^{-2} \text{ rad}$ |
| Δx_6 | $\dot{\psi}$ | $2.5^\circ \text{ s}^{-1} \approx 4.36 \times 10^{-2} \text{ rad s}^{-1}$ |
| Δx_7 | z | 0.025 m |
| Δx_8 | \dot{z} | 0.0125 m s^{-1} |
| Δx_9 | x | 0.05 m |
| Δx_{10} | \dot{x} | 0.025 m s^{-1} |
| Δx_{11} | y | 0.05 m |
| Δx_{12} | \dot{y} | 0.025 m s^{-1} |

Control weighting matrix. For the control input, we wish to minimize the use of excessive throttle. We can accomplish this by setting $\Delta u_i = 2^{-1/2} \omega_{\max}^2$ for $i \in [1, 4]$. This will translate to a maximum of $\pm 71\%$ throttle on each rotor, yielding a thrust cap at the [Root Mean Square \(RMS\)](#) value of the maximum thrust,

$T_{\text{cap}} = T_{\text{max}}/\sqrt{2}$, if we assume it to vary as a sinusoid. Similar to the state weighting matrix, the control weighting matrix will assume the form of:

$$\begin{bmatrix} \Delta u_1^{-2} & 0 & \dots & 0 \\ 0 & \Delta u_2^{-2} & \ddots & \vdots \\ \vdots & \ddots & \ddots & 0 \\ 0 & \dots & 0 & \Delta u_4^{-2} \end{bmatrix} \quad (7.4.3)$$

Summarizing, we obtain the following cost function:

$$\mathcal{J} = \rho \mathbf{x}^\top \mathbf{Q} \mathbf{x} + \mathbf{u}^\top \mathbf{Q}_2 \mathbf{u} \quad (7.4.4)$$

Part V

Safety

Chapter 8

Safety Plan Overview

The safety of all team members is of the absolute highest priority for the Illinois Space Society Student Launch team. Should a situation arise in which a project-critical choice needs to be made, safety is considered before the success of the project. The safety officer this year is Zana Essmyer, who is overseeing a small team to conduct a thorough analysis of any hazards the team may encounter this year throughout the design, construction, assembly, and launches of the rocket and payload. Zana and the safety team are also implementing plans and procedures to minimize the risk of associated hazards.

This year, using a combination of in-person briefings, online classes and thorough documentation, the team is actively encouraging participation in the adherence to safety procedures. Safety training is required for any member that wishes to participate in construction sessions or attend a launch. By keeping lists of safety-trained members and having experienced members actively involved at every build session, the team can ensure that everyone working in lab spaces understands safety protocol for both day-to-day work and potential emergency situations. Forthcoming checklists will also be developed to ensure total safety during the off-pad, on-pad and post flight procedures.

8.1 Emergency Preparedness

Though the Illinois Space Society strives to maintain a safe working environment during all phases of the competition, the team also recognizes that accidents remain a possibility even with the strictest safety precautions in place. With this in mind, emergency preparedness forms another pillar of the team's safety plan. First aid kits are easily accessible in all of the team's main workspaces, and the safety officer has familiarized herself with their contents. The kits themselves are up-to-date and include wound dressings, antibiotic ointments, painkillers, and antihistamines. For any injuries requiring more than basic first aid, medical facilities are available both on and off the University of Illinois campus.

8.2 Incident Reporting

In the rare event that an accident requiring first aid occurs, the primary goal is always to care for and assist the injured team member. That said, once the incident has passed, the safety team's next priority is to actively prevent accident reoccurrence. Any incident is to be reported immediately to the safety officer, and from there it will be her responsibility to speak to those involved and determine the exact cause of the accident. Review of an incident will be considered complete once the safety officer has surveyed the scenario to her satisfaction and offered recommendations to the team leadership on how to prevent similar incidents in the future.

If an incident happens to occur, a series of actions will enact. The non-injured team member will assess the situation for any immediate dangers before contacting the Safety Officer, Technical Manager, and, if needed, emergency personnel. The Safety Officer will document the incident. The safety team will then take action to prevent further incidents.

8.3 Equipment Training

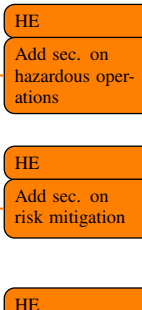
In order to provide team members with the experience necessary to operate a wide array of equipment and tooling, the safety team provides tutorial sessions on all machinery and tooling that may be used during the course of construction that is provided in the Nuclear Engineering Laboratory. To that end, the safety team has duplicated or adapted manufacturer-provided operating procedures for these tools and uploaded them to the team's shared drive for easy access. A collection of all training documents can be found in APPENDIX D: ISS Common Materials and Equipment Training with information included for the following devices:

- Full Spectrum Laser Professional Series CO2 48"×36" Cutter
- Ultimaker 2 Extended 3D Printer
- Milwaukee Sawzall Reciprocating Saw
- DeWalt 18V Wireless Power Drill
- Dremel 8200-1/28 12-Volt Max Cordless Rotary Tool
- G5000 RocketPoxy
- Grizzly Model G7297 12" Disc Sander
- Water-Cooled Diamond Table Saw
- Grizzly H2936 Vacuum Sanding Table
- GMC 16" Scroll Saw
- JET 15" Bench Drill Press
- Soldering Station
- Miscellaneous Hand Tools (Screwdrivers, Hammer, Clamps, etc.)

In order to operate this machinery, a team member must attend tutorial sessions or receive training separately from a member of the safety team or team management. In providing and requiring these sessions, the team not only reduces the risk of mishaps due to misuse of equipment, but also ensures redundancy in knowledge of construction techniques. The Safety Officer will host tutorial sessions for ESPL machinery at the beginning of the semester for all members before access will be granted.

8.4 NAR/Tripoli Rocketry Association (TRA) Procedures

The team will comply with the “High Power Rocket Safety Code” provided on the [NAR](#) website that has been effective since August 2012. The 13-step code and Minimum Distance Table on the website will be reviewed by the safety officer. All members on the team will be required to read the safety code online as it is a relatively short list of codes. The rules set forth by the [NAR](#) High Power Rocketry Code will always be respected and followed as they are set to ensure the safety of people and the environment. The safety officer, team manager, and sub-team managers will always make sure to comply with the safety code and ensure the rest of the team is properly complying. A copy of the [NAR](#) High Power Rocketry Code is included in this report as App. A. Additionally, sections and elaborate on the hazardous operations and mitigation of risks. Hazardous materials and proper protocol is detailed under section.



NAR Mentor. Mark Joseph will be the NAR mentor for the ISS Student Launch team for this year's competition. In addition to his longtime involvement in the high-power rocketry community, Mark has worked with the ISS team for several years now in the NASA Space Grant, Intercollegiate Rocket Engineering, and Student Launch Competitions.

Chapter 9

Risk Assessment Overview

To better prepare for issues that inevitably arise during any project of large scale and to prioritize the team's time, the safety team has conducted a thorough risk analysis based on incident severity. The safety team analyzed risks to the project, the environment, and above all, the health of team members during the construction process. The team used [Risk Assessment Codes \(RACs\)](#) to evaluate the various hazards to both personnel and the project. Table 9.1 introduces the risk matrix and the risk assessment codes that will be used to classify risks throughout the rest of the safety section. Risks are color-coded based on their severity, and discusses the team's response to these various levels. defines the levels of severity as it relates to personnel, project, and environmental health. Table 9 defines individual instance probability and probability of occurrence throughout the entire project timeline.

Table 9.1: Level of risk and member requirements

| Probability | Severity | | | |
|--------------|----------------|------------|------------|--------------|
| | 1—Catastrophic | 2—Critical | 3—Marginal | 4—Negligible |
| A—Frequent | 1A | 2A | 3A | 4A |
| B—Probable | 1B | 2B | 3B | 4B |
| C—Occasional | 1C | 2C | 3C | 4C |
| D—Remote | 1D | 2D | 3D | 4D |
| E—Improbable | 1E | 2E | 3E | 4E |

Part VI

Project Plan

Chapter 10

Budget

10.1 Structures and Recovery

| ID | Item | Purpose | Number | Unit Cost | Total Cost | Owned? |
|-----------|--------------------------------|---------------------------|---------------|------------------|-------------------|---------------|
| SR.1 | Epoxy and resin | Structural joints | N.A. | 70 USD | 70 USD | X |
| SR.2 | 60"×4" (L×W) Blue Tube | Upper and lower air-frame | 1 | 90 USD | 90 USD | ✓ |
| SR.3 | 12"×4" (L×D) Blue Tube coupler | Main rocket coupler bay | 1 | 45 USD | 45 USD | X |
| SR.4 | 9"×6" (L×D) Fiber-glass tube | Fairing tube | 1 | 60 USD | 60 USD | X |

Appendices

Appendix A

NAR High-Power Rocketry Safety Code

High Power Rocket Safety Code

Effective August 2012

1. Certification. I will only fly high power rockets or possess high power rocket motors that are within the scope of my user certification and required licensing.
2. Materials. I will use only lightweight materials such as paper, wood, rubber, plastic, fiberglass, or when necessary ductile metal, for the construction of my rocket.
3. Motors. I will use only certified, commercially made rocket motors, and will not tamper with these motors or use them for any purposes except those recommended by the manufacturer. I will not allow smoking, open flames, nor heat sources within 25-ft. of these motors.
4. Ignition System. I will launch my rockets with an electrical launch system, and with electrical motor igniters that are installed in the motor only after my rocket is at the launch pad or in a designated prepping area. My launch system will have a safety interlock that is in series with the launch switch that is not installed until my rocket is ready for launch, and will use a launch switch that returns to the “off” position when released. The function of onboard energetics and firing circuits will be inhibited except when my rocket is in the launching position.
5. Misfires. If my rocket does not launch when I press the button of my electrical launch system, I will remove the launcher’s safety interlock or disconnect its battery, and will wait 60 seconds after the last launch attempt before allowing anyone to approach the rocket.
6. Launch Safety. I will use a 5-second countdown before launch. I will ensure that a means is available to warn participants and spectators in the event of a problem. I will ensure that no person is closer to the launch pad than allowed by the accompanying Minimum Distance Table. When arming onboard energetics and firing circuits I will ensure that no person is at the pad except safety personnel and those required for arming and disarming operations. I will check the stability of my rocket before flight and will not fly it if it cannot be determined to be stable. When conducting a simultaneous launch of more than one high power rocket I will observe the additional requirements of NFPA 1127.
7. Launcher. I will launch my rocket from a stable device that provides rigid guidance until the rocket has attained a speed that ensures a stable flight, and that is pointed to within 20 degrees of vertical. If the

wind speed exceeds 5 miles per hour I will use a launcher length that permits the rocket to attain a safe velocity before separation from the launcher. I will use a blast deflector to prevent the motor's exhaust from hitting the ground. I will ensure that dry grass is cleared around each launch pad in accordance with the accompanying Minimum Distance table, and will increase this distance by a factor of 1.5 and clear that area of all combustible material if the rocket motor being launched uses titanium sponge in the propellant.

8. Size. My rocket will not contain any combination of motors that total more than 40,960 N-sec (9208 pound-seconds) of total impulse. My rocket will not weigh more at liftoff than one-third of the certified average thrust of the high power rocket motor(s) intended to be ignited at launch.
9. Flight Safety. I will not launch my rocket at targets, into clouds, near airplanes, nor on trajectories that take it directly over the heads of spectators or beyond the boundaries of the launch site, and will not put any flammable or explosive payload in my rocket. I will not launch my rockets if wind speeds exceed 20 miles per hour. I will comply with Federal Aviation Administration airspace regulations when flying, and will ensure that my rocket will not exceed any applicable altitude limit in effect at that launch site.
10. Launch Site. I will launch my rocket outdoors, in an open area where trees, power lines, occupied buildings, and persons not involved in the launch do not present a hazard, and that is at least as large on its smallest dimension as one-half of the maximum altitude to which rockets are allowed to be flown at that site or 1500-ft., whichever is greater, or 1000-ft. for rockets with a combined total impulse of less than 160 N-sec, a total liftoff weight of less than 1500 grams, and a maximum expected altitude of less than 610 meters (2000-ft.).
11. Launcher Location. My launcher will be 1500-ft. from any occupied building or from any public highway on which traffic flow exceeds 10 vehicles per hour, not including traffic flow related to the launch. It will also be no closer than the appropriate Minimum Personnel Distance from the accompanying table from any boundary of the launch site.
12. Recovery System. I will use a recovery system such as a parachute in my rocket so that all parts of my rocket return safely and undamaged and can be flown again, and I will use only flame-resistant or fireproof recovery system wadding in my rocket.
13. Recovery Safety. I will not attempt to recover my rocket from power lines, tall trees, or other dangerous places, fly it under conditions where it is likely to recover in spectator areas or outside the launch site, nor attempt to catch it as it approaches the ground.

Appendix B

Federal Aviation Regulations 14 CFR, Part 107, Small Unmanned Aircraft Regulations

The [Federal Aviation Authority \(FAA\)](#) rules for small unmanned aircraft (referred to as ‘[Unmanned Aerial Systems \(UASs\)](#)’) operations other than model aircraft—Part 107 of [FAA](#) regulations—cover a broad spectrum of commercial and government uses for [UAVs](#) weighing less than 55 pounds. This chapter lists the highlights of the rule.

Operating Requirements. When you are manipulating the controls of a drone, always avoid manned aircraft and never operate in a careless or reckless manner. You must keep your drone within sight. Alternatively, if you use [First Person View \(FPV\)](#) or similar technology, you must have a visual observer always keep your aircraft within unaided sight (for example, no binoculars). Neither you nor a visual observer can be responsible for more than one unmanned aircraft operation at a time.

You can fly during daylight (30 minutes before official sunrise to 30 minutes after official sunset, local time) or in twilight with appropriate anti-collision lighting. Minimum weather visibility is three miles from your control station. The maximum allowable altitude is 400 feet above the ground, higher if your drone remains within 400 feet of a structure. Maximum speed is 100 mph (87 knots).

You currently cannot fly a small [Unmanned Aerial System \(UAS\)](#) over anyone not directly participating in the operation, not under a covered structure, or not inside a covered stationary vehicle. No operations from a moving vehicle are allowed unless you are flying over a sparsely populated area.

You can carry an external load if it is securely attached and does not adversely affect the flight characteristics or controllability of the aircraft. You also may transport property for compensation or hire within state boundaries provided the drone, including its attached systems, payload and cargo, weighs less than 55 pounds total and you obey the other flight rules. (Some exceptions apply to Hawaii and the District of Columbia.)

You can request a waiver of most restrictions if you can show your operation will provide a level of safety at least equivalent to the restriction from which you want the waiver.

Registration. Anyone flying under Part 107 has to register each drone they intend to operate. If your drone weighs less than 55 lbm, you can use the automated registration system.

Pilot Certification. To operate the controls of a small [UAS](#) under Part 107, you need a remote pilot certificate with a small [UAS](#) rating, or be under the direct supervision of a person who holds such a certificate

You must be at least 16 years old to qualify for a remote pilot certificate, and you can obtain it in one of two ways.

You may pass an initial aeronautical knowledge test at an [FAA](#)-approved knowledge testing center.

If you already have a Part 61 pilot certificate, you must have completed a flight review in the previous 24 months and you must take a small [UAS](#) online training course provided by the [FAA](#).

If you have a Part 61 certificate, you will immediately receive a temporary remote pilot certificate when you apply for a permanent certificate. Other applicants will obtain a temporary remote pilot certificate upon successful completion of [Transportation Security Administration \(TSA\)](#) security vetting. We anticipate we will be able to issue temporary certificates within 10 business days after receiving a completed application.

UAS Certification. You are responsible for ensuring a drone is safe before flying, but the [FAA](#) does not require small [UAS](#) to comply with current agency airworthiness standards or obtain aircraft certification. For example, you will have to perform a preflight inspection that includes checking the communications link between the control station and the [UAS](#).

Other Requirements. If you are acting as pilot in command, you have to comply with several other provisions of the rule:

- You must make your drone available to the [FAA](#) for inspection or testing on request, and you must provide any associated records required to be kept under the rule.
- You must report any operation that results in serious injury, loss of consciousness, or property damage of at least \$500 to the [FAA](#) within 10 days

Waivers and Airspace Authorizations. The [FAA](#) can issue waivers to certain requirements of Part 107 if an operator demonstrates they can fly safely under the waiver without endangering other aircraft or people and property on the ground or in the air. Operations in Class G airspace are allowed without air traffic control permission. Operations in Class B, C, D and E airspace need [Air Traffic Control \(ATC\)](#) approval.

In November 2017, the [FAA](#) deployed the Low Altitude Authorization and Notification Capability (LAANC – pronounced “LANCE”) for drone operators at several air traffic facilities in an evaluation to see how well the prototype system functions and to address any issues that arise during testing. A beta test expansion of the system began on April 30, 2018 to deploy LAANC incrementally at nearly 300 air traffic facilities covering approximately 500 airports. The final deployment will begin on September 13.

The [FAA](#) expects LAANC will ultimately provide near real-time processing of airspace authorization requests for drone operators nationwide. The system is designed to automatically approve most requests to operate in specific areas of airspace below designated altitudes.

Appendix C

Federal Aviation Regulations 14 CFR, Subchapter F, Part 101, Subpart C – Amateur Rockets

§ 101.21 Applicability.

- (a) This subpart applies to operating unmanned rockets. However, a person operating an unmanned rocket within a restricted area must comply with § 101.25(b)(7)(ii) and with any additional limitations imposed by the using or controlling agency.
- (b) A person operating an unmanned rocket other than an amateur rocket as defined in § 1.1 of this chapter must comply with 14 CFR Chapter III.

§ 101.22 Definitions.

The following definitions apply to this subpart:

- (a) ***Class 1 - Model Rocket*** means an amateur rocket that:
 - (1) Uses no more than 125 grams (4.4 ounces) of propellant;
 - (2) Uses a slow-burning propellant;
 - (3) Is made of paper, wood, or breakable plastic;
 - (4) Contains no substantial metal parts; and
 - (5) Weighs no more than 1,500 grams (53 ounces), including the propellant.
- (b) ***Class 2 - High-Power Rocket*** means an amateur rocket other than a model rocket that is propelled by a motor or motors having a combined total impulse of 40,960 Newton-seconds (9,208 pound-seconds) or less.
- (c) ***Class 3 - Advanced High-Power Rocket*** means an amateur rocket other than a model rocket or high-power rocket.

§ 101.23 General operating limitations.

- (a) You must operate an amateur rocket in such a manner that it:

- (1) Is launched on a suborbital trajectory;

- (2) When launched, must not cross into the territory of a foreign country unless an agreement is in place between the United States and the country of concern;
- (3) Is unmanned; and
- (4) Does not create a hazard to persons, property, or other aircraft.

(b) The [FAA](#) may specify additional operating limitations necessary to ensure that air traffic is not adversely affected, and public safety is not jeopardized.

§ 101.25 Operating limitations for Class 2-High Power Rockets and Class 3-Advanced High Power Rockets.

When operating *Class 2-High Power Rockets* or *Class 3-Advanced High Power Rockets*, you must comply with the General Operating Limitations of § 101.23. In addition, you must not operate *Class 2-High Power Rockets* or *Class 3-Advanced High Power Rockets* -

- (a) At any altitude where clouds or obscuring phenomena of more than five-tenths coverage prevails;
- (b) At any altitude where the horizontal visibility is less than five miles;
- (c) Into any cloud;
- (d) Between sunset and sunrise without prior authorization from the [FAA](#);
- (e) Within 9.26 kilometers (5 nautical miles) of any airport boundary without prior authorization from the [FAA](#);
- (f) In controlled airspace without prior authorization from the [FAA](#);
- (g) Unless you observe the greater of the following separation distances from any person or property that is not associated with the operations:
 - (1) Not less than one-quarter the maximum expected altitude;
 - (2) 457 meters (1,500-ft.);
- (h) Unless a person at least eighteen years old is present, is charged with ensuring the safety of the operation, and has final approval authority for initiating high-power rocket flight; and
- (i) Unless reasonable precautions are provided to report and control a fire caused by rocket activities.

§ 101.27 ATC notification for all launches.

No person may operate an unmanned rocket other than a Class 1 - Model Rocket unless that person gives the following information to the [FAA ATC](#) facility nearest to the place of intended operation no less than 24 hours before and no more than three days before beginning the operation:

- (a) The name and address of the operator; except when there are multiple participants at a single event, the name and address of the person so designated as the event launch coordinator, whose duties include coordination of the required launch data estimates and coordinating the launch event;
- (b) Date and time the activity will begin;
- (c) Radius of the affected area on the ground in nautical miles;
- (d) Location of the center of the affected area in latitude and longitude coordinates;
- (e) Highest affected altitude;
- (f) Duration of the activity;
- (g) Any other pertinent information requested by the [ATC](#) facility.

§ 101.29 Information requirements.

(a) **Class 2 - High-Power Rockets.** When a *Class 2 - High-Power Rocket* requires a certificate of waiver or authorization, the person planning the operation must provide the information below on each type of rocket to the [FAA](#) at least 45 days before the proposed operation. The [FAA](#) may request additional information if necessary to ensure the proposed operations can be safely conducted. The information shall include for each type of Class 2 rocket expected to be flown:

- (1) Estimated number of rockets,
- (2) Type of propulsion (liquid or solid), fuel(s) and oxidizer(s),
- (3) Description of the launcher(s) planned to be used, including any airborne platform(s),
- (4) Description of recovery system,
- (5) Highest altitude, above ground level, expected to be reached,
- (6) Launch site latitude, longitude, and elevation, and
- (7) Any additional safety procedures that will be followed.

(b) **Class 3 - Advanced High-Power Rockets.** When a *Class 3 - Advanced High-Power Rocket* requires a certificate of waiver or authorization the person planning the operation must provide the information below for each type of rocket to the [FAA](#) at least 45 days before the proposed operation. The [FAA](#) may request additional information if necessary to ensure the proposed operations can be safely conducted. The information shall include for each type of Class 3 rocket expected to be flown:

- (1) The information requirements of paragraph (a) of this section,
- (2) Maximum possible range,
- (3) The dynamic stability characteristics for the entire flight profile
- (4) A description of all major rocket systems, including structural, pneumatic, propellant, propulsion, ignition, electrical, avionics, recovery, wind-weighting, flight control, and tracking,
- (5) A description of other support equipment necessary for a safe operation,
- (6) The planned flight profile and sequence of events,
- (7) All nominal impact areas, including those for any spent motors and other discarded hardware, within three standard deviations of the mean impact point,
- (8) Launch commit criteria,
- (9) Countdown procedures, and
- (10) Mishap procedures.

Bibliography

- [1] Dmitry Bershadsky, Steve Haviland, and Eric N. Johnson. Electric Multirotor UAV Propulsion System Sizing for Performance Prediction and Design Optimization. In *57th AIAA/ASCE/AHS/ASC Structures, Structural Dynamics, and Materials Conference*, San Diego, California, USA, January 2016. American Institute of Aeronautics and Astronautics. ISBN 978-1-62410-392-6. doi: 10.2514/6.2016-0581.
- [2] Justin Winslow, Vikram Hrishikeshavan, and Inderjit Chopra. Design Methodology for Small-Scale Unmanned Quadrotors. *Journal of Aircraft*, 55(3):1062–1070, May 2018. ISSN 0021-8669, 1533-3868. doi: 10.2514/1.C034483.
- [3] Abhishek Kumar Shastry, Mangal Kothari, and Abhishek Abhishek. Generalized Flight Dynamic Model of Quadrotor Using Hybrid Blade Element Momentum Theory. *Journal of Aircraft*, 55(5):2162–2168, September 2018. ISSN 0021-8669, 1533-3868. doi: 10.2514/1.C034899.
- [4] Mark Drela and Michael Giles. ISES - A two-dimensional viscous aerodynamic design and analysis code. In *25th AIAA Aerospace Sciences Meeting*, Reno,NV,U.S.A., March 1987. American Institute of Aeronautics and Astronautics. doi: 10.2514/6.1987-424.
- [5] J.B. Brandt, R.W. Deters, G.K. Ananda, and M.S. Selig. UIUC Propeller Database. <http://m-selig.ae.illinois.edu/props/propDB.html>, 2019.
- [6] 2020 NASA Student Launch Handbook and Request for Proposal. Handbook, Office of STEM Engagement NASA Marshall Space Flight Center, Huntsville, AL, August 2019.
- [7] Federal Aviation Administration. FAA Reauthorization Act of 2018, November 2018.
- [8] Raghubansh P. Singh, Louis C. P. Huang, and Roland A. Cook. SENS-5D Trajectory and Wind-Sensitivity Calculations for Unguided Rockets. Contractor Report, Computer Sciences Corporation, Wallops Island, VA, December 1975. Prepared under Contract No. NAS6-2369 for Wallops Flight Center, Wallops Island, VA.
- [9] Lior M. Burko and Richard H. Price. Ballistic trajectory: Parabola, ellipse, or what? *American Journal of Physics*, 73(6):516–520, June 2005. doi: 10.1119/1.1866097.
- [10] Sevkuthan Kurak and Migdat Hodzic. Control and Estimation of a Quadcopter Dynamical Model. *Periodicals of Engineering and Natural Sciences (PEN)*, 6(1):63, March 2018. ISSN 23034521. doi: 10.21533/pen.v6i1.164.
- [11] Pedro Castillo, Laura Elena Muñoz Hernández, and Pedro García Gil. *Indoor Navigation Strategies for Aerial Autonomous Systems*. Butterworth-Heinemann, Oxford, 2017. ISBN 978-0-12-805189-4. OCLC: ocn958449100.

- [12] Teppo Luukkonen. Modelling and control of quadcopter. Independent research, Aalto University, School of Science, Espoo, Finland, August 2011.
- [13] A. Tayebi and S. McGilvray. Attitude stabilization of a four-rotor aerial robot. In *2004 43rd IEEE Conference on Decision and Control (CDC) (IEEE Cat. No.04CH37601)*, pages 1216–1221 Vol.2, Nassau, Bahamas, 2004. IEEE. ISBN 978-0-7803-8682-2. doi: 10.1109/CDC.2004.1430207.
- [14] Gene F. Franklin, J. David Powell, and Michael L. Workman. *Digital Control of Dynamic Systems*. Addison-Wesley, Menlo Park, Calif., 3rd ed. edition, 2002. ISBN 978-0-201-82054-6 978-0-201-33153-0. OCLC: 249361424.